Bathymetry and geographical regionalization of Brepollen (Hornsund, Spitsbergen) based on bathymetric profiles interpolations

Mateusz MOSKALIK[1], Piotr GRABOWIECKI[1], Jarosław TĘGOWSKI[2]
and Monika ŻULICHOWSKA[3]

[1] *Instytut Geofizyki, Polska Akademia Nauk, ul. Księcia Janusza 64, 01-452 Warszawa, Poland*
<mmosk@igf.edu.pl> <graba@igf.edu.pl>

[2] *Wydział Oceanografii i Geografii, Uniwersytet Gdański,*
Al. M. Piłsudskiego 46, 81-378 Gdynia, Poland <j.tegowski@ug.edu.pl>

[3] *Wydział Biologii i Nauk o Ziemi, Uniwersytet Jagielloński,*
ul. Gronostajowa 7, 30-387 Kraków, Poland <m_zulik@interia.pl>

Abstract: Determination of High Arctic regions bathymetry is strictly dependent from weather and ice mass quantity. Due to safety, it is often necessary to use a small boat to study fjords area, especially close to glaciers with unknown bathymetry. This precludes the use of modern multi-beam echosounders, and so traditional single-beam echosounders have been used for bathymetry profiling. Adequate interpolation techniques were determined for the most probable morphological formations in-between bathymetric profiles. Choosing the most accurate interpolation method allows for the determination of geographical regionalisation of submarine elevations of the Brepollen area (inner part of Hornsund, Spitsbergen). It has also been found that bathymetric interpolations should be performed on averaged grid values, rather than individual records. The Ordinary Kriging Method was identified as the most adequate for interpolations and was compared with multi beam scanning, which was possible to make due to a previously modelled single beam interpolation map. In total, eight geographical units were separated in Brepollen, based on the bathymetry, slope and aspect maps. Presented results provide a truly new image of the area, which allow for further understanding of past and present processes in the High Arctic.

Key words: Arctic, Svalbard, Hornsund, bathymetry, kriging interpolation.

Introduction

Digital Elevation Model (DEM) analyses are widely used in Remote Sensing in order to obtain accurate topographical features of the area. With submarine DEM it is possible to monitor the dynamic morphology of the seabed, especially in

bays and fjords, which are under the constant forces of seawater currents, sedimentation and erosion processes connected with melting glaciers. Acoustic study of a seabed offers non-invasive methods for more detailed understanding of past and present events.

New acoustic analysing methods (sub-bottom profilers, multi-beam and side scan sonar data) and measuring technology development provided new opportunities for even more precise submarine elevation models. Such models include information regarding geometry, morphology and types of forms built by glacial processes, sedimentation processes and the marine environment as well as seabed parameters such as types of sediments. Usage of multi-beam echosounders allows for acquiring seabed information in a short period of time. Recently in the Spitsbergen area these types of devices were used to obtain seabed morphology (*e.g.*, Dowdeswell *et al.* 2010; Forwick *et al.* 2009; Ottesen and Dowdeswell 2006, 2009; Ottesen *et al.* 2007, 2008). Such activities involve high financial expenses and introduce various limitations. Usually, due to safety risks, the surveys are conducted in the areas covered by officially published marine services (*e.g.*, The Norwegian Hydrographic Service and Norwegian Polar Research 1990; United Kingdom Hydrographic Office 2007) or navigation maps (*e.g.*, Statens Kartverk 2008). However, the above publications do not include areas where glaciers retreated, or where presented information is not detailed enough (Pastusiak 2010), and therefore it was required to run surveys in such areas from small boats, easy to navigate on shallow waters.

The poor level of information around Brepollen and its continued expansion connected with revealing new, hitherto inaccessible terrains from melting ice-cover, are the main imperatives driving the presented research, and render the obtained results of great significance. Detailed recognition of bottom morphology in connection with knowledge about the glacial genesis of the region will help better understanding of glacial processes and their reflection in various morphological forms. Certainly, it will also initiate and enable commencement of new research projects in the area of Brepollen.

Study area

The Hornsund, which is the southernmost major fjord developed in the west coast of Spitsbergen, is oriented along W-E direction and is about 30 km long (Fig. 1). According to the data published by Rudowski and Marsz (1998) the mean depth of Hornsund fjord basin is 93 m and the maximum 262 m. A strongly developed coastline forms five bays inside the fjord, all bounded with tidewater glaciers (Görlich 1986). The easternmost and therefore innermost of them is Brepollen Bay.

Brepollen is located between 76°59' and 77°01' N and 16°16' and 16°31' E. It is about 13 km long and its width varies from 1.7 km to 15 km. The mouth of the
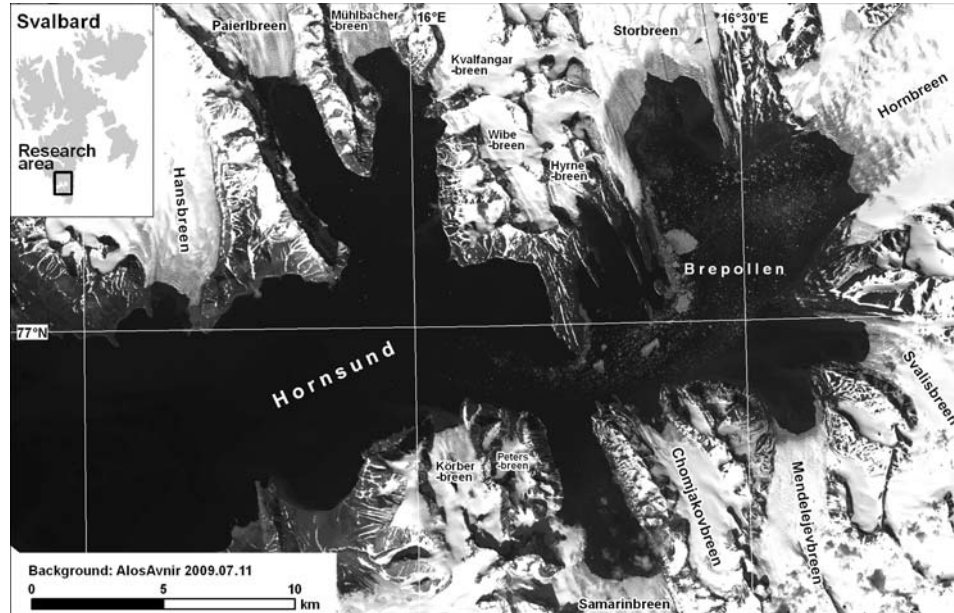
Fig. 1. Map of Hornsund, Svalbard (Alos Avnir © JAXA [2011]).

bay is formed by two capes: Treskelodden from the north and Meranpynten from the south. Within Brepollen several smaller, inner bays, developed especially in the ice cliffs of tidewater glaciers. In the northern and eastern parts of Brepollen the bays are separated by peninsulas. The biggest ones are situated on the axes of Mezenryggen and Ostrogradskifjella massifs and bound Hornbreen glacier from the north and the south respectively. In the southern part of Brepollen glaciers' valleys are separated by longitudinal mountain massifs (Fig. 1).

Tidewater glaciers, distinctive in the Svalbard environment, constitute for more than 60% of total ice-cover of the archipelago. They cover the vast majority of Brepollen so that the significant part of its coastline takes the form of ice cliffs. There are six tidewater glaciers flowing into Brepollen terminating in the form of a strongly crevassed ice cliff: Hyrnebreen (NW), Storbreen (N), Hornbreen (NE), Svalisbreen (SE), Mendelejevbreen (S) and Chomjakovbreen (S). Their flow velocities vary from very slow (5 m/yr) to fast (250 m/yr). The total length of ice cliffs in Brepollen was estimated at *ca* 18 400 m where the longest one, 7 690 m in length belonged to Storbreen glacier (Błaszczyk *et al.* 2009).

The shape and area of Brepollen are directly influenced by the fluctuation of tidewater glaciers' fronts. Previous research indicates that glaciers of Hornsund, like the ones in Brepollen, have diminished in extent and thickness during the last century, and are retreating with different intensities due to their individual characteristics (Głowacki and Jania 2008; Kolondra 2010). According to Głowacki and Jania (2008) the fjord was growing in average by *ca* 1 km²/yr from the beginning

of 20th century until the middle 1980's. This rate increased to 1.8±0.5 km²/yr in the last decade. It is estimated that the mean recession rate of Hornsund glaciers varies from *ca* 10 m/yr for small cirque glaciers to *ca* 20–50 m/yr for tidewater glaciers (Głowacki and Jania 2008), but according to Sneed (2007) and Pälli *et al.* (2003) the 50–100 years average recession rates of Hornbreen and Storbreen account for *ca* 140–160 m/yr. In Brepollen the incidental surge of Mendelejewbreen in 2000 was observed (Błaszczyk *et al.* 2010). Rapid recession and volume reduction of Hornbreen and Hambergbreen glaciers' system during the 20th century became a reason for developing the hypothesis of the existence of a continuous sub-sea-level channel connecting Hornsund with the Barents Sea. Nevertheless, ground-penetrating radar surveys revealed that Hornbreen-Hambergbreen system bed lies at -25 to 25 m above sea level and there is continuous connection between Torell Land and Sørkapp Land (Pälli *et al.* 2003).

Most of bottom morphology surveys in Brepollen were taken for general bathymetry mapping purposes and bottom sediments identification. The measurements were performed using various echo-sounders and seismo-acoustic apparatus during polar expeditions of the Institute of Geophysics, Polish Academy of Sciences between 1976 and 1991, but the average depth of Brepollen has never been investigated, and so far no bathymetric maps have been produced for the area.

Materials and methods

Equipment and data acquisition

Bathymetric data were collected using low-cost remote sensing system, during the summer months of 2007 and 2008. The measurements were performed from a small boat equipped with a Lowrance LMS-527cDF type echosounder, coupled with a GPS receiver. This is the single beam echosounder which operates in two frequencies (50/200 kHz) and widths of 35°/12° respectively. The system is not recommended for navigation but it can provide the data to create the bathymetry model for environmental analyses (Goluch *et al.* 2010; Heyman *et al.* 2007). This type of echo-sounding equipment, an implemented methodology for determining reservoir depths, assumes a constant speed of sound in water of 1462.992 m/s (4800 ft/s). Collected data was exported to text format, containing information regarding the depth (in feet) and the geographical position as defined by Lowrance-Mercator coordinates (LMC).

With the device, 95 bathymetry profiles were created in 2007 totalling 217 km in length and more than 255 thousands measurements of depth. In 2008, 25 profiles of 167 km in length and almost 280 thousands depth measurements were obtained (Fig. 2). The measurements were performed on a boat cruising at the speed of 3 to 8 km/h, relative to the reservoir bottom.
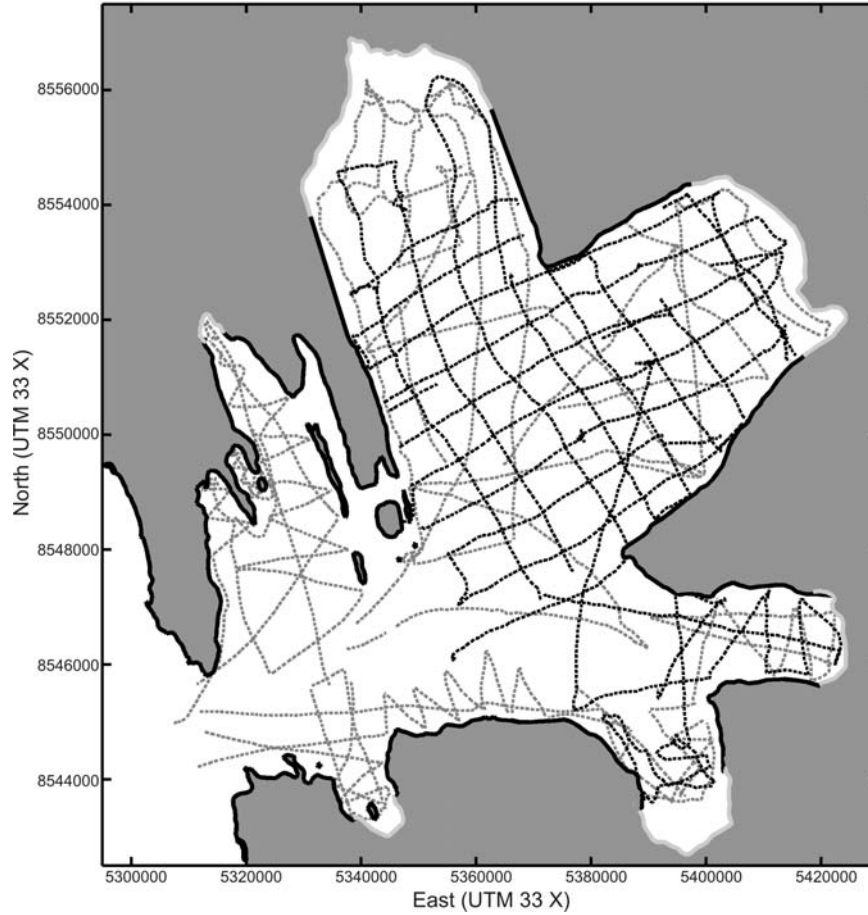
Fig. 2. Bathymetric profiles locations during 2007 (grey dashed line) and 2008 (black dashed line) at Brepollen, Spitsbergen.

Data pre-processing

LMC were calculated to geographical positions using the formula (Heyman *et al.* 2007):

$$Lon = \frac{180}{\pi} \cdot \frac{LMC_E}{b}$$

$$Lat = \frac{180}{\pi} \left(2 \cdot \arctan \left(\exp \left(b \frac{LMC_N}{} \right) \right) - \frac{\pi}{2} \right)$$

(1)

where: *Lon*, *Lat* – Longitude and Latitude in degree, LMC_E, LMC_N – Easting and Northing LMC, $b \approx 6356752.31$ – polar radius of Earth in meters. Geographical position in degrees was transformed to Universal Transverse Mercator (UTM) coordinates.

Bathymetric data collected by the echosounder contained two major groups of errors:

- errors generated by GPS during the time of registration and the geographical location,
- errors generated by the echosounder software affecting determination of depth.

Incorrect coordinates occurred due to the absence of information obtained from a GPS receiver. The lack of information resulted from a greater emission of acoustic signals sent, rather than the ones received from satellites by GPS system. The most common errors in depth measurements were caused by non-turbulent sea water flows around the emitter. This caused dispersion and attenuation of the signal and slow speed cruising was not always effective. Some overestimations of depths were also caused by echoes produced by sound multi reflections of seafloor scatters.

For data pre-processing and error correction, in the first step, the incorrect geographical localisation was removed. Spatial geographical localisation gaps were interpolated afterwards. Another interesting issue was the depth correction on bathymetric profiles. The most appropriate way to avoid wrong depth interpretation by echo-sounder software was to apply filters, which removed incorrectly specified depths. Such issues were discussed (White 2003; White and Hodges 2005) where usage of median filtration (MF) was suggested. MF replaces values by median of values included in MF window. As there was a risk of replacing the true value, authors suggested to modify the filter and introduced parameter definition, as an absolute difference between the measured value and the value after MF. If the parameter exceeded a set limit, it qualified the measured data as invalid. The main issue in such analysis was to validate and set the correct size for the MF window and identification of a set value. Most of the gaps in the data sets are from a few hundred meters to few kilometres. MF window size was set as double the distance of the lowest data gaps and was set to 100 m. A value for identification of valid depths was set as 3 times the standard deviation of measured depths in the MF window. Such approach allowed elimination of incorrect values on steep slopes or high peaks.

Statistical approach

During in-field works in Brepollen area more than 530 000 measurements depth values (MDV) were collected. The maximum depth from MDV exceeded 145 m and the shallowest recorded areas had less than 0.5 m. The average depth value calculated from MDV was almost 36 m, while median as approx. 30 m. The mode – the most frequent measured value, was calculated as approx. 8 m. Left-skewed distribution was equal to -1.11. Kurtosis, defined as:

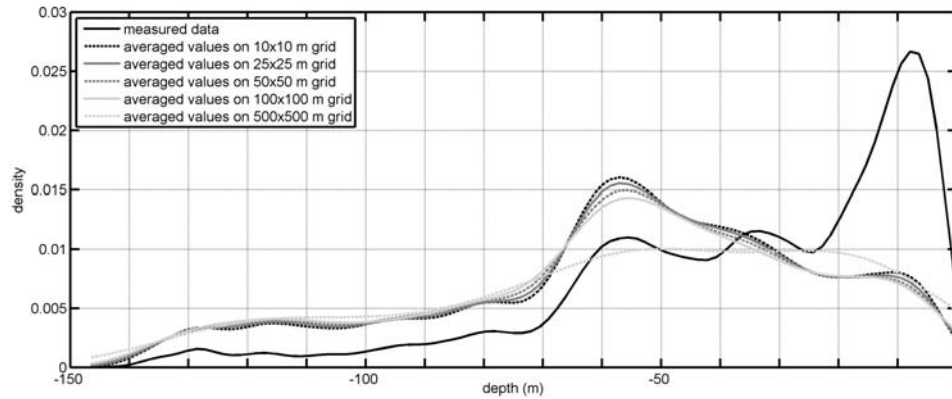$$Kurt_x = \frac{\frac{1}{N}\sum_{i-1}^{N}\left(x_i - x_{av}\right)^4}{\sigma_x^4} - 3 \qquad (2)$$

Fig. 3. Depth distributions from bathymetric records and averaged values on 10, 25, 100 and 500 m grid.

where: x_i – measured depth value; x_{av} – average depth value; N – the number of records; σ_x – standard deviation, was 0.94 for MDV. Density Distribution (DD) was varying and it was not easily described by any density function (Fig. 3). At least 3 local maxima at intervals of 5–10, 30–40 and 50–60 m were identified.

These statistical parameters were compared with the parameters assigned to the Averaged Depth Values (ADV) on grids with 10, 25, 50 and 100 m size (Table 1). For all ADV analogous distributions in values were observed, although on 500 m grid it was noticed that local extreme values were smoothed, which resulted in one maximum – close to the average value of all the records. The DD for depth lower than 30 m was reduced and for higher than 60 m was increased for all ADV compared to MDV (Fig. 3). For the ADV the differences between average, median and mode value were reduced in comparison to analogue MDV parameters. It was noticed that the value of kurtosis decreased when the grid size increased. The skewness stays negative and for all ADV are similar. Considering this information, it was decided that calculated ADV would be used for further analysis.

Table 1

Values used in statistical analysis based on bathymetric recorded during 2007 and 2008 seasons and averaged grid values of 10, 25, 50, 100 and 500 m.

	Measured values	Averaged values on a grid size of:				
		10×10 m	25×25 m	50×50 m	100×100 m	500×500 m
Mean (m)	−35.9	−56.0	−56.5	−57.0	−57.5	−55.0
Median (m)	−29.6	−53.0	−53.3	−53.7	−54.1	−51.4
Dominant (m)	−8	−58	−58	−57	−56	−51
Standard deviation (m)	29.6	33.0	32.9	33.1	33.6	35.9
Skewness	−1.11	−0.57	−0.56	−0.53	−0.51	−0.52
Kurtosis	0.94	−0.27	−0.32	−0.38	−0.43	−0.72
Maximum depth (m)	−145.2	−145.1	−144.4	−143.4	−141.7	−139.2
Minimum depth (m)	−0.4	−0.5	−0.5	−0.8	−0.8	−2.3

Data interpolations

Range of interpolation. — Data interpolation can provide the value estimation at any point in the area. Interpolated value is calculated using known neighbouring data. General linear interpolation formula can be written as:

$$x_{int} = \sum_i w_i \cdot x_i$$
$$\forall_{i,|x_i,x_{int}|>RoI} w_i = 0 \tag{3}$$
$$\sum_i w_i = 1$$

where: x_{int} – the interpolated value, x_i – the value of a known parameter, w_i – interpolation weights, *RoI* – range of interpolation.

The highest distance between profiles is lower than 1000 m. Minimal *RoI* where the whole Brepollen area was to be interpolated, should be higher than 500 m, half of the maximal distance. Brepollen's valleys (in size) are higher than 500 m on a few occasions, and such estimation could be too high. Herzfeld *et al.* (1995) discussed that bathymetry could be designed as a regionalised variable. Based on this information semivariogram was used for the description of correlation between neighbouring depth values and calculated *RoI*. The empirical semivariogram was calculated from the equation:

$$\gamma(h) = \frac{\sum \left[z(x) - z(x+h) \right]^2}{2n} \tag{4}$$

where: *z(x), z(x+h)* – values in locations in the distance of *h*; *n* – number of point pairs in the distance of *h*.

Theoretical models of semivariograms are characterized by a few parameters. For the analysis, the most important was the range of semivariation, which describes the distance of decreasing correlation between the values.

Figure 4A presents semivariogram calculated for AGV on 100 m grid. It was clear that the range of the semivariogram may be estimated as 4000–5000 m. With such distances, depths from opposite coastlines could be included in the calculations, which made the semivariogram unrealistic. At this stage of the analysis it was important to determine the actual extent and so, a semivariogram for a 10 m grid was plotted (Fig. 4B). The change in increase of semivariation, was clear on the derivative of semivariation $d(\gamma(h))/dh$ plot (Fig. 4C) in the range of 400 to 500 m. Based on this, the *RoI* was established as 500 m.

Excerpts from theory of used interpolation methods. — Groups of fitting polynomial functions, inverse distance weights and kriging methods were used for interpolation bathymetry in the Brepollen area. These methods have been discussed and used for interpolation of topographic and other GIS environmental data in many published works (*e.g.*, Chaplot *et al.* 2006; James 1996; Krivoruchko
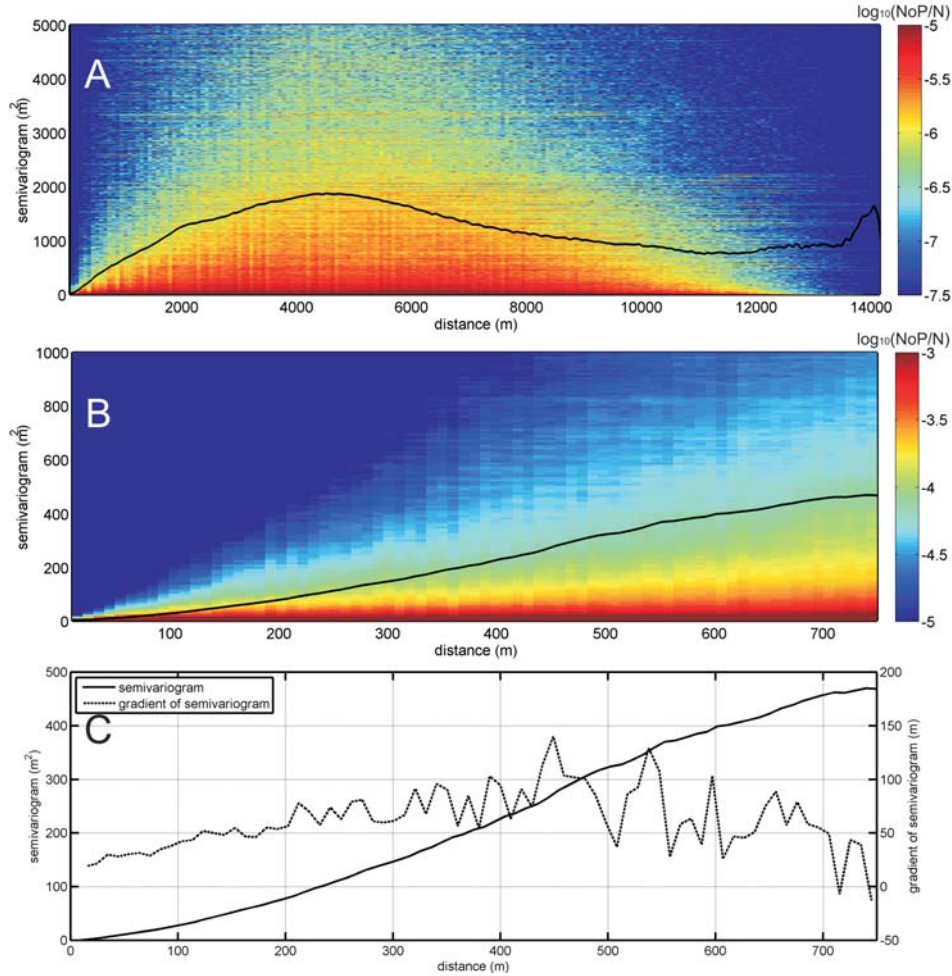
Fig. 4. Number of pair (semivariation, distance) in logarithmic scale with empirical semivariogram (black line) based on the averaged data on 100 m grid (A), 10 m grid (B) and semivariogram with its derivative for 10 m grid (C). Figure in color available in the online version.

2001; Legleiter and Kyriakidis 2008; Merwade 2009; Majdański 2012; Moskalik and Bialik 2011; Moskalik *et al.* 2012; Schmidt *et al.* 2003).

The first interpolation method was fitting a polynomial function to known values (PolM). It can be described by *N*-stage polynomial:

$$P(x, y)_N = \sum_{j=i}^{N} \sum_{i=0}^{N} A_{Nij} x^i y^j \tag{5}$$

In case of N=1 (PolM1) and N=2 (PolM2), the Equation 5 looks as follows:

$$P(x, y)_1 = A_{110} x + A_{101} y + A_{100} \tag{6}$$

$$P(x, y)_2 = A_{220} x^2 + A_{202} y^2 + A_{211} xy + A_{210} x + A_{201} y + A_{200} \tag{7}$$

Using the least square method, parameters A_{Nij} were calculated, minimizing the sum of squares of differences between known values in known locations $Z(X,Y)$, and the value of interpolated pane $P(X,Y)_N$. Therefore the method can be described as browsing for the minimum value of function:

$$x^2 = \sum_{X,Y}\left(Z(X,Y) - \sum_{j=i}^{N}\sum_{i=0}^{N} A_{Nij} X^i Y^j \right)^2 \qquad (8)$$

The issue can be solved by calculating simultaneous equations:

$$\forall_{A_{Nij}} \; \frac{\partial \chi^2}{\partial A_{Nij}} = 0 \qquad (9)$$

which for $N = 1$, is

$$\begin{vmatrix} \sum X^2 & \sum XY & \sum X \\ \sum XY & \sum Y^2 & \sum Y \\ \sum X & \sum Y & N \end{vmatrix} \cdot \begin{vmatrix} A_{110} \\ A_{101} \\ A_{100} \end{vmatrix} = \begin{vmatrix} \sum XZ \\ \sum YZ \\ \sum Z \end{vmatrix} \qquad (10)$$

and for $N = 2$, is

$$\begin{vmatrix} \sum X^4 & \sum X^2 Y^2 & \sum X^3 Y & \sum X^3 & \sum X^2 Y & \sum X^2 \\ \sum X^2 Y^2 & \sum Y^4 & \sum XY^3 & \sum XY^2 & \sum Y^3 & \sum Y^2 \\ \sum X^3 Y & \sum XY^3 & \sum X^2 Y^2 & \sum X^2 Y & \sum XY^2 & \sum XY \\ \sum X^3 & \sum XY^2 & \sum X^2 Y & \sum X^2 & \sum XY & \sum X \\ \sum X^2 Y & \sum Y^3 & \sum XY^2 & \sum XY & \sum Y^2 & \sum Y \\ \sum X^2 & \sum Y^2 & \sum XY & \sum X & \sum Y & N \end{vmatrix} \cdot \begin{vmatrix} A_{220} \\ A_{202} \\ A_{211} \\ A_{210} \\ A_{201} \\ A_{200} \end{vmatrix} = \begin{vmatrix} \sum ZX^2 \\ \sum ZY^2 \\ \sum XZY \\ \sum XZ \\ \sum YZ \\ \sum Z \end{vmatrix} \qquad (11)$$

It is important to note, that with PoIM methods it is possible to extrapolate calculated values outside the minimum and the maximum range, used during interpolation. The main disadvantage of the methods is generating amplitudes between the measuring nodes, which in reality could be non-existent. This is especially clear, when dealing with higher polynomials. The method of interpolation through the designation of the mean values from known values (MIM), is a specific example for parameter $N = 0$.

The second group of methods used was inverse distance weights (IDW) and can be presented as follows:

$$w_i = \frac{1/r_i^k}{\sum_{j=i}^{N} 1/r_j^k} \text{ for k} \geq 0 \qquad (12)$$

where r_i – distance between interpolated and known value; k – exponent index defining method; N – number of values used during interpolation.

The interesting cases occur when exponent index $k = 0$ and $k = \infty$. In the first case the interpolated values are calculated as mean of known values (MIM – Mean Interpolated Method). The more interesting is the second case where the exponent k inclines to infinity:

$$x_{\text{int}} = \sum_i (x_i / r_j^k) / \sum_{j=1}^{N} 1 / r_j^k = \sum_i \left((r_{\min} / r)^k x_i \right) / \sum_{j=1}^{N} (r_{\min} / r_j)^k =$$

$$\sum_{\forall_i, r_i \neq r_{\min}}^{N} \left((r_{\min} / r)^k x_i \right) / \sum_{j=1}^{N} (r_{\min} / r_j)^k + x_{i, r_i = r_{\min}} / \left(1 + \sum_{\forall_i, r_i \neq r_{\min}}^{N} \left((r_{\min} / r_j)^k \right) \right) \xrightarrow{k \to \infty} x_{i, r_i = r_{\min}} \quad (13)$$

It must be noted from Equation 13, that this methodology is the same as the Nearest Neighbours Method (NNM). With IDW methods it is impossible to extrapolate beyond maximum and minimum values. IDW methods with k taken as: 0 (MIM), 0.25 (IDW1/4), 0.5 (IDW1/2), 1 (IDW1), 2 (IDW2), 4 (IDW4) and infinity (NNM) were used.

The last group of methods were kriging methods. In Ordinary Kriging (OKM) weights are calculated from equations:

$$\begin{pmatrix} \gamma(d_{11}) & \gamma(d_{12}) \ldots \gamma(d_{1n}) & 1 \\ \gamma(d_{21}) & \gamma(d_{22}) \ldots \gamma(d_{2n}) & 1 \\ \vdots & \vdots \quad \ddots \quad \vdots & \vdots \\ \gamma(d_{n1}) & \gamma(d_{n2}) \ldots \gamma(d_{nn}) & 1 \\ 1 & 1 \quad \ldots \quad 1 & 0 \end{pmatrix} \cdot \begin{pmatrix} w_1 \\ w_2 \\ \vdots \\ w_n \\ \lambda \end{pmatrix} = \begin{pmatrix} \gamma(d_{1\,\text{int}}) \\ \gamma(d_{1\,\text{int}}) \\ \vdots \\ \gamma(d_{1\,\text{int}}) \\ 1 \end{pmatrix}, \text{ or } A\,w = b \quad (14)$$

where: $\gamma(d_{ij})$ – theoretical semivariogram value for i-th and j-th points, $\gamma(d_{i\,\text{int}})$ – theoretical semivariogram value for i-th and interpolated point, λ –Lagrange coefficient, w_i – weight for i-th value of the parameter.

If the determinant of the matrix A is a non-zero, the solution of the equation can be written as:

$$w = A^{-1} b \quad (15)$$

where A^{-1} is the inverse matrix of A. Standard deviation of OKM is described as:

$$\sigma_{\text{int}} = \left(\sum_j w_j \cdot \gamma(d_{j\,\text{int}}) + \lambda \right)^{0.5} \quad (16)$$

The modification of OKM is a Universal Kriging (UKM), which assumes the existence of trend in the data. In such a case it is not the values being determined, but the difference between recorded value and the ones determined from the trend. Two polynomial trends was used, first (UKM1) and second (UKM2) stages.

The results, choice of the method and its verifications

The results

Figure 5 provides the results of all used interpolation methods on 25 m grid. The following characteristics of each interpolation methods were identified from those examples and other results of interpolation on 10, 50 and 100 m grids:

– In the result of interpolation, the appearance of discontinuity in bathymetry data occurred, when using PolM1, PolM2, UKM1 and UKM2 methods. If the location of known values was close to each other, but the differences between them were considerable, the interpolated values, based on polynomial fitting, may greatly differ from each other.
– In the result of the PoIM2 method, more detailed information about bathymetry was obtained, than in the PoIM1 method.
– In the result of the interpolation IDW methods, the increase of bathymetry details was linked with the growing of the exponent index. This was the result of faster declining influence of known values with the distance.
– NNM methods result in rapid changes in interpolated values. Such "jumps" in depths cannot be considered as realistic, since in most cases the seabed topography is characterised as a continuity function.
– In the result of kriging with interpolations on 10 m grid size, some data gaps are observed in the calculated datasets. Those gaps are also shown on Fig. 6. These gaps were for determination of the matrix A equal zero.
– Standard deviations of kriging were close to zero in the survey profiles and it grew with the increase of the distance from the profiles. Growth was faster in the slopes than on the flat sea beds. Standard deviations of kriging was higher for larger grid sizes (Fig. 6).
– The standard deviations were smaller for UKM, than for OKM.

Choice of the method

In order to indicate one method of interpolation authors suggested using the following criteria:

– calculate sensitivity of the methods on the grid size;
– compliance of the distribution of the results of interpolation with distribution of input value;
– visual assessment and rejection of the methods which give unrealistic values.

The last criterion was the results of subjective evaluation presented above and methods such NNM, PolM1, PolM2, UKM1 and UKM2 were worse than MIM, IDW1/4, IDW1/2, IDW1, IDW2, IDW4 and OKM. The first two criteria derive from mathematical analysis of interpolation results and are presented below.

It was assumed that ideal method of interpolation should provide the same results regardless of the interpolation grid size. In order to examine the results of the
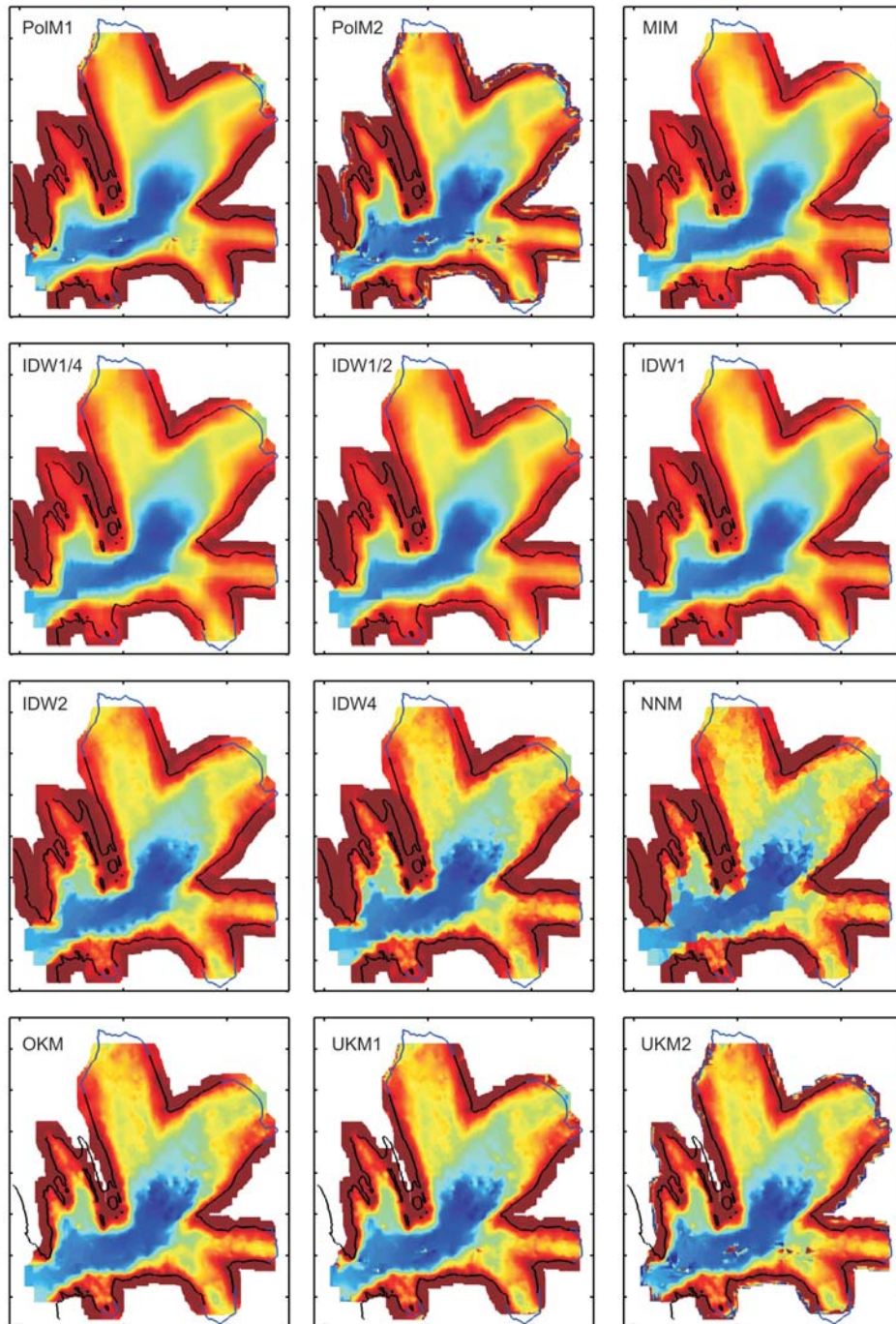
Fig. 5. Bathymetric interpolations visualisation of Brepollen, calculated with all methods on 25 m grid size – explained in detail in the text. Depth range: -145 m (blue) to 0 m (red). Figure in color available in the online version.
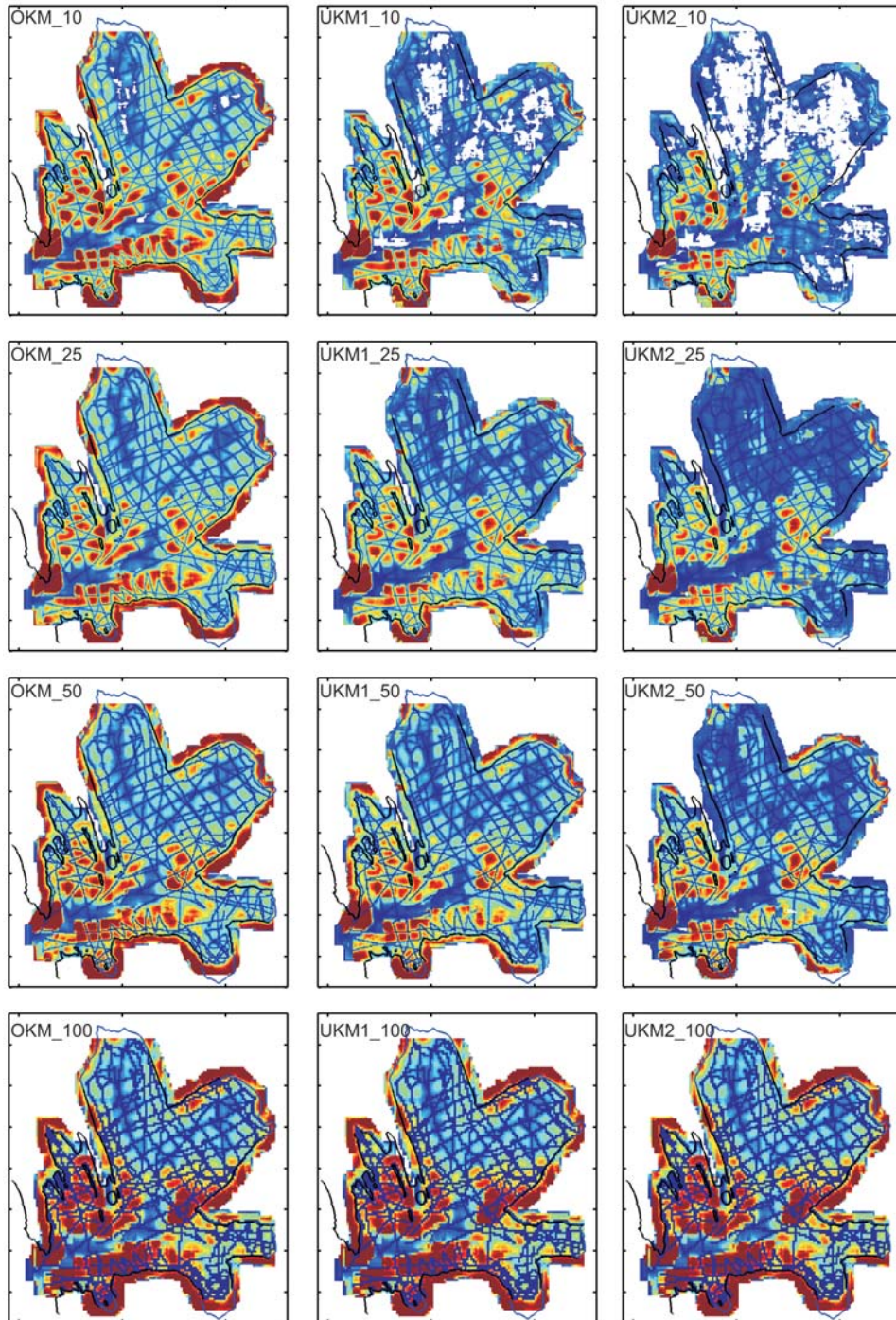
Fig. 6. Standard deviation of kriging methods with variable grid sizes – explained in detail in the text. Standard deviation range: 0 m (blue) to 10 m (red). Figure in color available in the online version.

study it was proposed to analyse the distance between point (Xin_{25}, Xin_{50}, Xin_{100}), defined by the interpolated depths for different grid size in all localization, from a straight line $X_1 = X_2 = X_3$, the theoretical consistent values line. Interpolation maps of 10 m grid size were not used due to gaps when kriging methods were used. The distance can be written as:

$$d_{in2cv} = \sqrt{R^2 - 3 \cdot \overline{X_{in}}^2} \qquad (17)$$

where

$$R = \sqrt{X_{in25}^2 + X_{in50}^2 + X_{in100}^2} \qquad (18)$$

and $\overline{X_{in}}$ – average interpolated value.

In order to analyse the interpolation methods the cumulative distribution function, the density of probability (Fig. 7) statistical parameters (Table 2) of d_{in2cv} were prepared for all of the interpolated methods.

From analyzes of median and mean values of d_{in2cv}, it was possible to conclude that the best fitting was obtained with MIM and IDW methods with exponent lower than 1, because these parameters were the lowest. The least suitable results were calculated using UKM and PoIM methods, and the worse methods were the ones, where second degree polynomials were used.

Another criterion for choosing interpolation method is to examine the dominants of the density function of d_{in2cv}. Null dominant is typical for NNM method. This is due to the nature of this interpolation method, where the interpolated value is the nearest known value. Dominants of density function increases from 0.10 to 0.35 in

Table 2

Parameters of statistical analysis of distances between point defined by the interpolated depths for different grid size from consistent values line for every interpolation method.

|	Parameter	Mean (m)	Median (m)	Dominant (m)	Standard deviation (m)	Skewness	Kurtosis	Minimum value (10–15 m)	Maximum value (m)
	PolM1	2.67	1.16	0.34	6.1	8.0	96	0	178
	PolM2	8.03	1.49	0.43	41.8	22.8	956	0	3566
	MIM	1.41	0.92	0.35	1.7	4.1	37	0	58
Interpolation method	IDW1/4	1.40	0.91	0.34	1.7	4.0	38	0	58
	IDW1/2	1.38	0.91	0.33	1.6	4.0	38	0	58
	IDW1	1.42	0.93	0.34	1.6	3.6	33	0	57
	IDW2	1.67	1.03	0.32	2.0	3.0	18	0	56
	IDW4	1.87	1.03	0.10	2.6	3.8	24	0	55
	NNM	2.88	1.1	0.00	5.7	5.8	50	0	88
	OKM	1.96	1.24	0.46	2.3	3.8	27	0	43
	UKM1	2.99	1.55	0.47	5.4	7.9	108	1.7	177
	UKM2	8.01	1.75	0.55	40.9	24.1	1060	2.9	3564
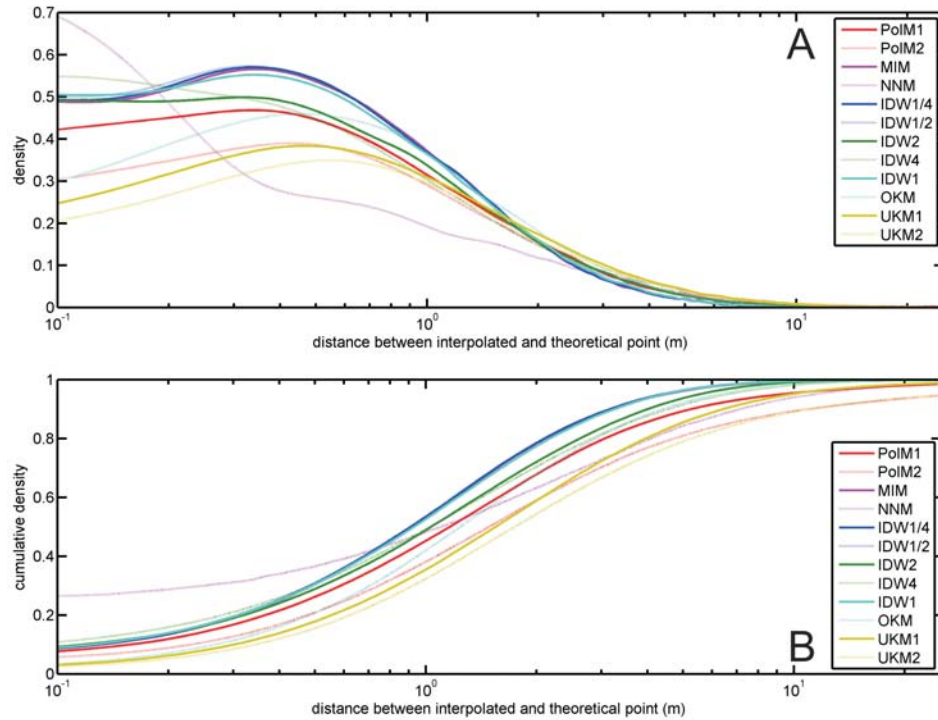
Fig. 7. Distribution function (**A**) and cumulative density (**B**) of distance between point defined by the interpolated depths for different grid size from consistent values line for every interpolation method. Figure in color available in the online version.

IDW methods when the exponent index is decreasing (from 4 to 0 for MIM). Usage as a dominant factor, determining the sensitivity of the interpolation method for grid size, indicates that kriging methods (both OKM and UKM) were not the best ones.

Apart from upper criteria, the maximum values of compliance could be used, for the dependency of interpolations on grid sizes. The lowest maximum occurs in the OKM method. The least suitable methods using such approach were found to be UKM and PolM.

Summarizing analyses of d_{in2cv} parameter as criteria to chose interpolation methods, the IDW and OKM methods were suggested.

In the last step for choosing interpolation methods, it was assumed that distribution of the measured depths was representative for the research area. For choosing interpolation methods, the distribution of the results of interpolation with distribution of input value was compared. For this purpose, the cumulative sum of absolute difference in the distribution of the interpolated values and the values applied for interpolation was determined. The lowest anomalies from the measured values were found in PolM, NNM, OKM and UKM methods.

As a conclusion of the above analyses the OKM method was chosen for bathymetry interpolation to characterise Brepollen submarine morphology.

Single beam methods verification

In order to verify above the calculation, and choosing Ordinary Kriging for interpolation, bathymetric datasets from OKM on 25 × 25 meter grid (Fig. 8) hes been compared with information about bathymetry from multibeam echosounding surveying. Discussed datasets where obtained by two research groups. The first group from University of Tromsø, Norway, ran seabed scanning on r/v *Jan Mayen* in 2007 in the central Brepollen area (Forwick 2007) described on navigation charts. In 2010 the second group, from the Institute of Geophysics, Polish Academy of Sciences on Gdynia Maritime University r/v *Horyzont II*, updated information from 2007 surveys. 2010 scans were possible due to a previously modelled single beam interpolation map (Fig. 8). From both surveys, it was possible to obtain bathymetry of almost all Brepollen without costal zone with depths lower then over a dozen meters.
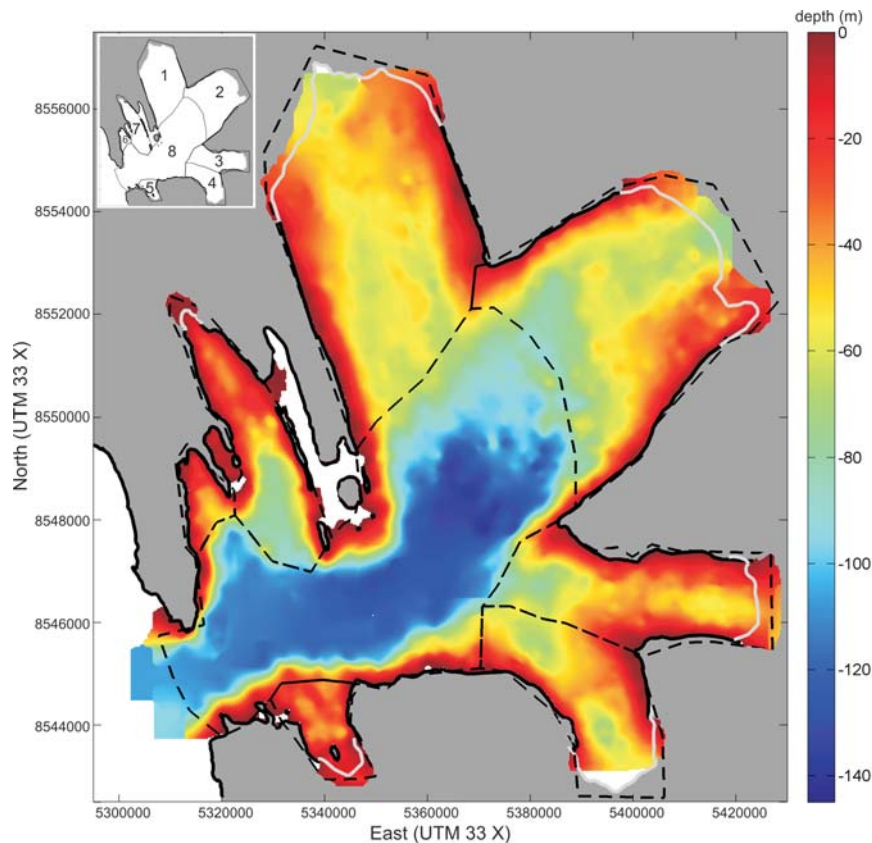

Fig. 8. Bathymetry of Brepollen calculated with OKM interpolation on 25 m grid and geographical regionalisation in Brepollen. Coastline in black; glaciers' reach in 2010 in grey; determined Brepollen bay regions – thin dashed black line. Determined geographical units: 1 – Storbreen glacier valley, 2 – Hornbreen glacier valley, 3 – Svalisbreen glacier valley, 4 – Mendelejevbreen glacier valley, 5 – Chomjakovbreen glacier valley, 6 – Treskelbukta Bay, 7 – Hyrnebreen glacier valley, 8 – Central Brepollen. Figure in color available in the online version.
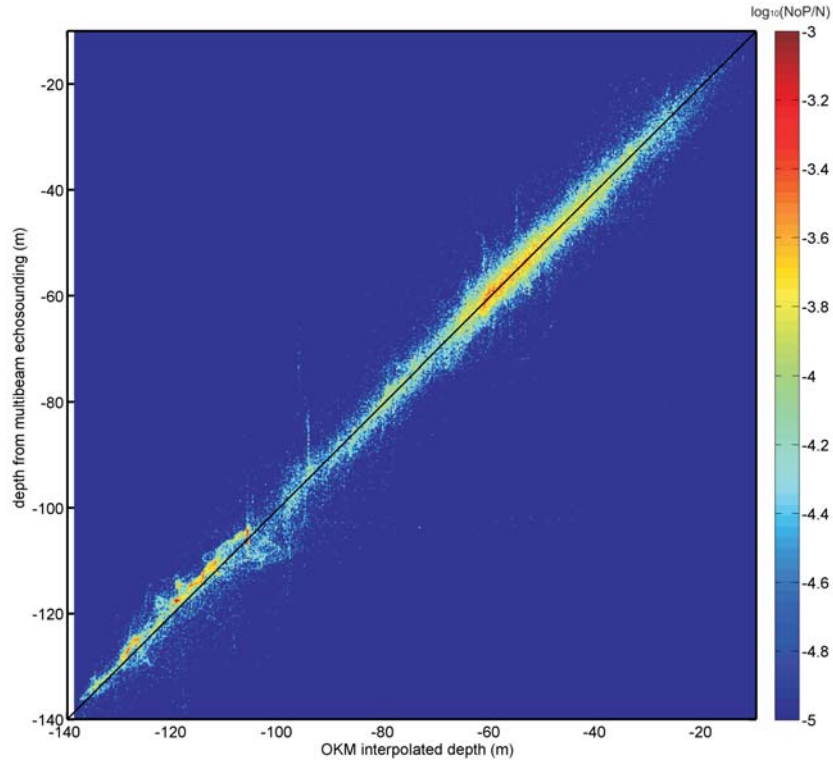
Fig. 9. Number of pair of depths obtained from OKM bathymetry and multibeam survey in specific localization in logarytmic scale and compatible depth (black line). Figure in color available in the on-line version.

By comparing depth from single beam OKM modelling with multi beam scans, it was possible to calculate a correlation coefficient of 0.98 (Fig. 9). Such high depth correlations were confirmed by distribution of absolute values of their subtraction where 0.25, 0.5 and 0.75 quantiles were equal to 0.9, 1.9 and 3.8 m respectively. The highest number of coincident pairs was obtained at a depth of up to 80 m. With the depth increase over 100 m, interpolated values were overstated, although lower than 2–3 m. This was due to the application of constant speed of sound in water in singlebeam bathymetry, as opposed to using a profile of sound speed for multibeam data processing, known from CTD profiles. The speed of sound decreased with depth from more then 1455 m/s close to surface to lower then 1445 m/s on almost 100 m (measured during 2010 survey).

Brepollen bathymetry maps: results and discussion

For the morphological analysis an additional two-dimensional median filter has been applied to the acquired image. Such approach allows for the elimination
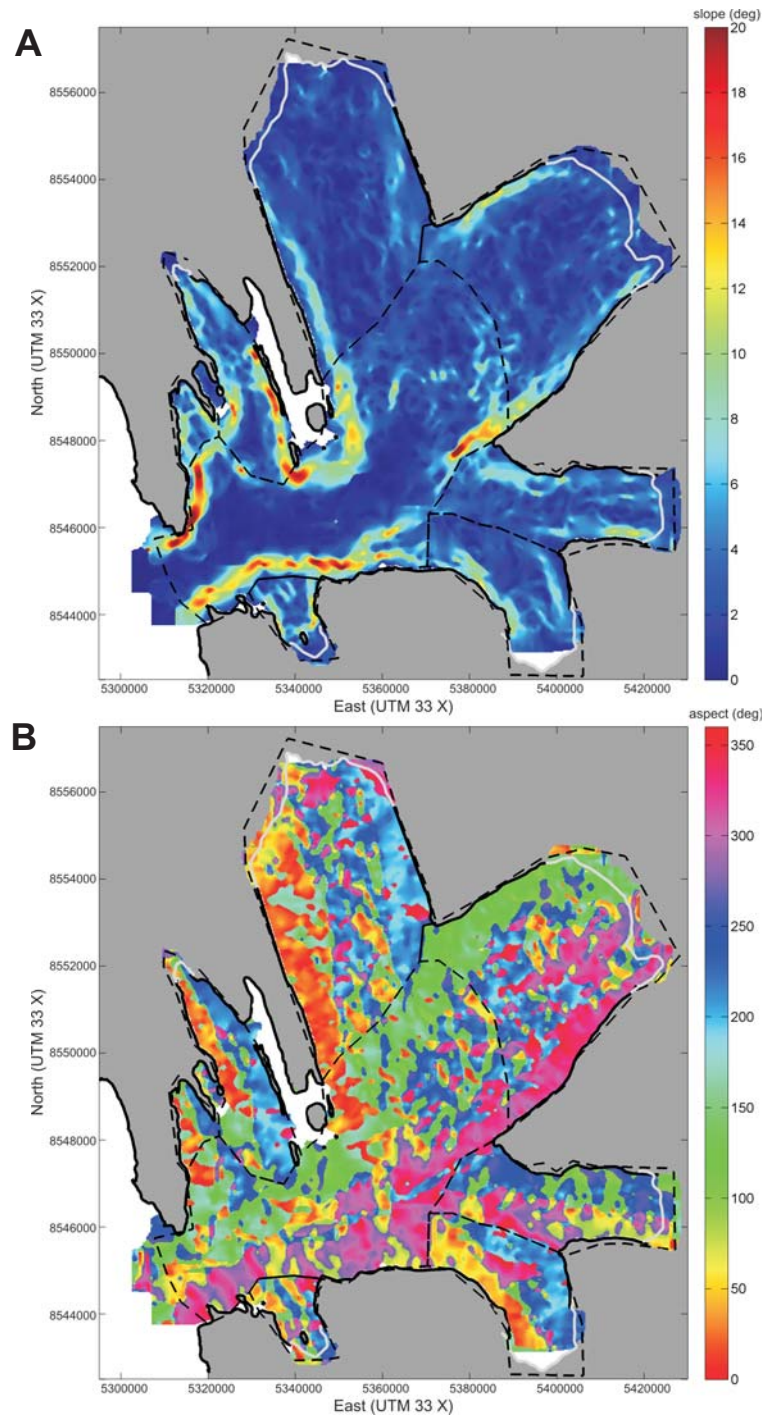
Fig. 10. Slope (**A**) and aspect (**B**) in Brepollen (based on bathymetric map on Fig. 8; legend as on Fig. 8). Figure in color available in the online version.

of significant depth variance, which could have significant impact in future analysis. Also, null and greater than zero values, were rejected. The results after filtration are presented on Fig. 8. Based on the bathymetry, slope and the aspect grids (Fig. 10A, B) further maps were produced (Moskalik *et al.* 2012).

Based on such information it was possible to define geographical regions in the area of Brepollen (Fig. 8). Eight units were defined in total, which include six postglacial valleys including existing glaciers (units 1–5 and 7); Treskelbukta Bay, a separated bay close to eastern part of Treskellen (unit 6) and central part of Brepollen (unit 8). All geographical units were determined by two major features:

– the boundaries of the geographical units are at the beginning of valleys' slope (Fig. 10A);
– the boundaries between the two units, which are in contact with each other are drawn due to uneven directions of the maximum slope decline (Fig. 10B).

Analyzing archival materials concerning the position of the glaciers' fronts in the years 1930–1960 (Głowacki and Jania 2008), it can be postulated that after their recession into the Brepollen in this period in Treskelbukta was a small independent glacier (Fig. 8). The central part of Brepollen (unit 8) was separated from the Storbreen glacier valley (unit 1) with a clear aspect, which allows for the conclusion that it makes up a direct extension of the Hornbreen glacier valley (unit 2) where its border is not so clear. The border has been set due to considerable sea bed differentiation in the eastern part of Brepollen, in the form of a few East-West ridges. In addition to these units, an additional small bay can be identified on the western side of unit 7 and non-surveyed area, between units 6 and 1 with a few islands and peninsulas.

In terms of the largest area, over 30% is dedicated to the central part of Brepollen (unit 8). The next largest areas are the Storbreen (unit 1) and Hornbreen (unit 2) glaciers valleys, a total of almost 40% of the Brepollen. The other five units including the smallest, Treskelbukta Bay, constitute less than 25% of the entire region. The non-classified regions constitute slightly over 5% of the area. Maximum depths with exceedance of 140 m can be found in the central part of Brepollen (unit 8). Depths higher than 100 m exist also in the southern part of the Hyrnebreen glacier valley (unit 7). In the postglacial valleys of Hornbreen and Storbreen glaciers, maximum depths were determined at more than 90 m and almost 70 m, respectively. In addition some notable depths were calculated for Svalisbreen (approx. 90 m, unit 3) and Mendelejevbreen valleys (approx. 80 m, unit 4).

Conclusions

In total 12 interpolation methods were tested on 4 grid sizes of 10x10 m, 25x25 m, 50x50 m and 100x100 m. The best method of interpolation and optimal grid size was found to be OKM with 25 m grid size, following from the elimination of other methods. The lower grid size 10 m was worse than 25 m because some data gaps are observed in the calculated datasets. In addition the comparison of sin-

gle beam interpolations with multi beam scanning confirmed the correctness of obtained results with an acceptable margin of error. Attention to the range of inter-polated areas should also be considered as these directly influence, the accuracy of interpolation; wrongly interpreted interpolation range can lead to the inclusion of opposite coastlines' data, when interpolating *i.e.* fjord or bays. For the area of Brepollen, it was possible to define 8 geographical units based on bathymetric in-terpolation, slope and aspect grids. This research confirms also, that the usage of single beam echosounders allow for introductory research of submarine elevation modelling in unknown and hard-to-reach areas.

References

BŁASZCZYK M., JANIA J.A. and HAGEN J.O. 2009. Tidewater glaciers of Svalbard: Recent changes and estimates of calving fluxes. *Polish Polar Research* 30 (2): 85–142.

CHAPLOT V., DARBOUX F., BOURENNANE H., LEGUEDOIS S., SILVERAAND N. and PHACHOMPHON K. 2006. Accuracy of interpolation techniques for the derivation of digital elevation models in relation to landform types and data density. *Geomorphology* 77: 126–141.

DOWDESWELL J.A., HOGAN K.A., EVANS J., NOORMETS R., O'COFAIGH C. and OTTESEN D. 2010. Past ice-sheet flow east of Svalbard inferred from streamlined subglacial landforms. *Geology* 38 (2): 163–166.

FORWICK M. 2007. *Marine-geological cruise to west Spitsbergen fjords*. Cruise Report N-9037. De-partment of Geology, University of Tromsø: 21 pp.

FORWICK M., BAETEN N.J. and VORREN T.O. 2009. Pockmarks in Spitsbergen fjords. *Norwegian Journal of Geology* 89: 65–77.

GŁOWACKI P. and JANIA J.A. 2008. Nature of rapid response of glaciers to climate warming in Southern Spitsbergen, Svalbard. In: *The First International Symposium on the Arctic Research, Drastic Change under Global Warming*. Miraikan, Tokyo: 257–260.

GOLUCH P., DOMBEK A. and KAPLON J. 2010. Evaluation of data accuracy obtained from bathy-metric measurement using fishinder Lowrance LMS-527C DF iGPS. *Archiwum Fotogrametrii, Kartografii i Teledetekcji* 21: 109–118 (in Polish).

GÖRLICH K. 1986. Glacimarine sedimentation of muds in Hornsund fjord, Spitsbergen. *Annales Societatis Geologorum Poloniae* 56: 433–477.

HERZFELD U.C., KIMAND I.I. and ORCUTT J.A. 1995. Is the Ocean Floor a Fractal? *Mathematical Geology* 27 (3): 421–462.

HEYMAN W.D., ECOCHARDAND J.-L.B. and BIASI F.B. 2007. Low-cost bathymetric mapping for tropical marine conservation – a focus on reef fish spawning aggregation sites. *Marine Geodesy* 30: 37–50.

JAMES L.A. 1996. Polynomial and power functions for glacial valley cross-section morphology. *Earth Surface Processes and Landforms* 21: 413–432.

KOLONDRA L. 2010. *Satellite orthophotomap of a part of South Spitsbergen, Svalbard*. University of Silesia, Faculty of Earth Sciences, Sosnowiec.

KRIVORUCHKO K. 2001. Using linear and non-linear kriging interpolators to produce probability maps. *In*: *Annual Conference of the International Association for Mathematical Geology (IAMG 2001)*, Cancun, Mexico. http://faculty.mu.edu.sa/public/uploads/1338413539.2214GIS30.pdf.

LEGLEITER C.J. and KYRIAKIDIS P.C. 2008. Spatial prediction of river channel topography by kriging. *Earth Surface Processes and Landforms* 33: 841–867.

MAJDAŃSKI M. 2012. The structure of the crust in TESZ area by Kriging interpolation. *Acta Geophysica* 60 (1): 59–75.

MERWADE V. 2009. Effect of spatial trends on interpolation of river bathymetry. *Journal of Hydrology* 371: 169–181.

MOSKALIK M. and BIALIK R.J. 2011. Statistical analysis of topography of Isvika Bay, Murchisonfjorden, Svalbard. *In*: P. Rowiński (ed.) *GeoPlanet: Earth and Planetary Sciences, Experimental Methods in Hydraulic Research, 1st ed.* Springer, Berlin Heidelberg: 225–233.

MOSKALIK M., PASTUSIAK T. and TĘGOWSKI J. 2012. Multi beam bathymetry and slopes stability of Isvika Bay, Murchisonfjorden, Nordaustlandet. *Marine Geodesy* 35 (4): 389–398.

OTTESEN D. and DOWDESWELL J.A. 2006. Assemblages of submarine landforms produced by tidewater glaciers in Svalbard. *Journal of Geophysical Research* v. 111, F01016.

OTTESEN D. and DOWDESWELL J.A. 2009. An inter-ice-stream glaciated margin: Submarine landforms and a geomorphic model based on marine-geophysical data from Svalbard. *Geological Society of America Bulletin* 121: 1647–1665.

OTTESEN D., DOWDESWELL J.A., LANDVIK J.Y. and MIENERT J. 2007. Dynamics of the Late Weichselian ice sheet on Svalbard inferred from high-resolution sea-floor morphology. *Boreas* 36: 286–306.

OTTESEN D., DOWDESWELL J.A., BENN D.I., KRISTENSEN L., CHRISTIANSEN H.H., CHRISTENSEN O., HANSEN L., LEBESBYE E., FORWICK M. and VORREN T.O. 2008. Submarine landforms characteristic of glacier surges in two Spitsbergen fjords. *Quaternary Science Reviews* 27: 1583–1599.

PASTUSIAK T. 2010. Issues of non-researched marine regions coverage by electronic maps. *Logistics, transportation systems, safety in transport* 2: 2069–2086 (in Polish).

PÄLLI A., MOORE J.C., JANIA J.A. and GŁOWACKI P. 2003. Glacier changes in southern Spitsbergen, Svalbard, 1901–2000. *Annals of Glaciology* 37: 219–225.

RUDOWSKI S. and MARSZ A. 1998. Characteristics of bottom relief and deposit cover in contemporary developing fjord on the example of Hornsund (Spitsbergen) and Admiralty Bay (West Antarctica). *In*: A. Styszyńska (ed.) *Research of Faculty of Navigation of Gdynia Maritime University*, Vol. III, WSM Academic Publishing, Gdynia: 39–81 (in Polish).

SCHMIDT J., EVANSAND I.S. and BRINKMANN J. 2003. Comparison of polynomial models for land surface curvature calculation. *International Journal of Geographical Information Science* 17 (8): 797–814.

SNEED W.A. 2007. *Satellite remote sensing of arctic glacier – climate interactions*. MSc dissertation, University of Maine, Orono: 83 pp.

Statens Kartverk 2008. *Paper chart 526, Hornsund, scale 1:50 000*. Statens kartverk Sjø, Stavanger.

The Norwegian Hydrographic Service and Norwegian Polar Research Institute 1990. *Den Norske Los. Arctic Pilot*, Vol. 7, 2nd edition: 433 pp.

United Kingdom Hydrographic Office. 2007. *NP11 Arctic Pilot Edition 2004*, 2007 Correction.

WHITE L. 2003. *Rivers bathymetry analysis in the presence of submerged large woody debris*. Master of Engineering dissertation, The University of Texas, Austin: 157 pp.

WHITE L. and HODGES B.R. 2005. Filtering the signature of submerged large woody debris from bathymetry data. *Journal of Hydrology* 309: 53–65.